International Journal of Nanomedicine

Dovepress
open access to scientific and medical research

Open Access Full Text Article

ORIGINAL RESEARCH

RETRACTED ARTICLE: Paclitaxel-Loaded Macrophage Membrane Camouflaged Albumin Nanoparticles for Targeted Cancer Therapy

This article was published in the following Dove Press journal:
International Journal of Nanomedicine

Xi Cao[1,2]
Tingfei Tan[1,2]
Dongchun Zhu[1,2]
Haixia Yu[1,2]
Yaru Liu[1,2]
Haiyun Zhou[1,2]
Yong Jin[3,4]
Quan Xia[1,2]

[1]Department of Pharmacy, The First Affiliated Hospital of Anhui Medical University, Hefei, People's Republic of China; [2]The Grade 3 Pharmaceutical Chemistry Laboratory of State Administration of Traditional Chinese Medicine, Hefei, People's Republic of China; [3]Key Laboratory of Anti-Inflammatory and Immune Medicines, Ministry of Education, School of Pharmacy, Anhui Medical University, Hefei, People's Republic of China; [4]Key Laboratory of Major Autoimmune Diseases, Anhui Province, Anhui Institute of Innovative Drugs, School of Pharmacy, Anhui Medical University, Hefei, People's Republic of China

Background: Melanoma is the most common symptom of aggressive skin cancer, and it has become a serious health concern worldwide in recent years. The metastasis rate of malignant melanoma remains high, and it is highly difficult to cure with the currently available treatment options. Effective yet safe therapeutic options are still lacking. Alternative treatment options are in great demand to improve the therapeutic outcome against advanced melanoma. This study aimed to develop albumin nanoparticles (ANPs) coated with macrophage plasma membranes (RANPs) loaded with paclitaxel (PTX) to achieve targeted therapy against malignant melanoma.

Methods: Membrane derivations were achieved by using a combination of hypotonic lysis, mechanical membrane fragmentation, and differential centrifugation to empty the harvested cells of their intracellular components. The collected membrane was then physically extruded through a 400 nm porous polycarbonate membrane to form macrophage cell membrane vesicles. Albumin nanoparticles were prepared through a well-studied nanoprecipitation process. At last, the two components were then coextruded through a 200 nm porous polycarbonate membrane.

Results: Using paclitaxel as the model drug, PTX-loaded RANPs displayed significantly enhanced cytotoxicity and apoptosis rates compared to albumin nanoparticles without membrane coating in the murine melanoma cell line B16F10. RANPs also exhibited significantly higher internalization efficiency in B16F10 cells than albumin nanoparticles without membrane coating. Next, a B16F10 tumor xenograft mouse model was established to explore the biodistribution profiles of RANPs, which showed prolonged blood circulation and selective accumulation at the tumor site. PTX-loaded RANPs also demonstrated greatly improved antitumor efficacy in B16F10 tumor-bearing mouse xenografts.

Conclusion: Albumin-based nanoscale delivery systems coated with macrophage plasma membranes offer a highly promising approach to achieve tumor-targeted therapy following systemic administration.

Keywords: macrophage membrane, albumin nanoparticles, melanoma, paclitaxel, tumor-targeted therapy

Introduction

Melanoma is a malignancy deriving from melanocytes, and the most common symptom is aggressive skin cancer.[1,2] In recent years, the incidence of malignant melanoma has continued to increase, and it has become a serious health concern worldwide.[3,4] Additionally, the metastasis rate of malignant melanoma remains high, and it is highly difficult to cure with the currently available treatment options.[5] With the rapid advances in cancer diagnostics and treatment options, early stage melanoma

Correspondence: Quan Xia
Tel +86 551 62922154
Email xiaquan2010@163.com

submit your manuscript | www.dovepress.com
DovePress
http://doi.org/10.2147/IJN.S244849

is often curable after surgery, while advanced melanoma remains challenging to treat.[4,6] Ipilimumab, dabrafenib, trametinib, and vemurafenib are the first-line therapeutic drugs for advanced melanoma; however, side effects are commonly observed, and the cost of treatment remains exceedingly high.[7] Thereby, alternative treatment options are in great demand to improve the therapeutic outcome against advanced melanoma.

Over the past few decades, nanoscale delivery systems have become a popular research topic for the targeted therapy of solid tumors. Nanoparticles have high drug-loading capacity, good storage stability, enhanced cytotoxicity, and may circumvent the multidrug resistance in tumor cells.[8–11] With a well-designed nanoparticle shell, drug-loaded nanoparticles are indicated to prolong the circulation of small molecule drugs in the blood circulation, which could facilitate the extravasation and passive targeting to the tumor site with an enhanced permeability and retention effect.[11,12] To achieve tumor-targeted drug delivery, a common strategy is to modify nanoparticles with targeting ligands such as antibodies and peptides.[13–15] These targeting ligands could bind with the receptors specifically overexpressed in cancer cells and mediate targeted delivery. Chen et al fabricated anisamide-modified cationic liposomes to systemically deliver small interfering RNA to treat melanoma, and the anisamide could bind with Sigma 1 receptors associated with melanoma cells to mediate the specific delivery of cargos to the tumor cells. However, problems such as the complex chemistry involved in the modification step remain to be explored, as well as how nanoparticles can escape from the rapid clearance by the reticuloendothelial system and achieve prolonged circulation.

Recently, increasing attention has been focused on the nanocarrier delivery system coated with different membranes for targeted disease therapy.[16–20] For example, cancer cell membrane-coated nanoparticles have been used for anticancer vaccination and drug delivery.[21] Erythrocyte-platelet hybrid membrane-coated nanoparticles successfully prolonged the circulation time of nanoparticles in vivo.[22] Moreover, emtansine liposomes coated with macrophage membranes were demonstrated to improve delivery to cancer metastatic sites.[20] With the increasing knowledge of cancer biology, some inflammatory factors have been recognized as associated with malignant growth, which may further promote and enhance tumor progression.[23] Neutrophils can be recruited to the inflammation site in response to a granulocyte colony-stimulating factor in the inflammatory microenvironment of the tumor.[24,25] A recent study demonstrated that neutrophil-mimicking nanoparticles could effectively inhibit the formation of cancer metastatic niches by targeting the circulating cancer stem cells.[26] Moreover, Xue et al reported that viable neutrophils carrying paclitaxel-loaded liposomes successfully suppressed postoperative glioma recurrence.[27] However, there are no reports available on the treatment of melanoma using such strategies.

Here, we reported albumin nanoparticles coated with macrophage plasma membranes as a means to achieve targeted therapy against malignant melanoma. Among a number of nanocarriers, albumin nanoparticles have received great attention in both academia and industry due to their noticeable advantages as pharmaceutical carrier, including biodegradability, biocompatibility, high chemical stability, and versatility and nonimmunogenicity (human source).[28–30] In particular, albumin nanoparticles could preferentially accumulate in tumor sites due to their remarkable targetability to tumors.[31] They penetrate leaky blood vessels via an efficient extravasation process.[32] Thus, whether the coating of plasma membrane can improve the uptake efficiency and targeting therapy of albumin nanoparticles remains to be explored. Paclitaxel (PTX) is a white crystalline powder isolated from the Pacific Yew (*Taxus brevifolia*). It is one of the most effective chemotherapeutics and is mainly used to treat lung cancer, ovarian cancer, and breast cancer;[33–35] however, its high toxicity and insolubility in aqueous solution limit its applications. In this study, albumin nanoparticles loaded with PTX (ANPs/PTX) were fabricated and decorated with macrophage membranes (RANPs/PTX). The cellular uptake efficiency of RANPs in different kinds of tumor cells, including B16F10 cells, MCF-7 cells, 4T1 cells, and A549 cells, was characterized. The uptake efficiencies were significantly improved among these cells, and murine B16F10 melanoma was chosen as the disease model to explore the treatment efficiency of the preparations. The in vitro antitumor effect of RANPs/PTX was evaluated in terms of cytotoxicity, cell cycle, and apoptosis rate in B16F10 cells. To evaluate the tumor-specific accumulation of RANPs, a biodistribution study in a tumor-bearing mouse xenograft model was also performed. Moreover, we preliminarily explored the antitumor efficacy against melanoma in the B16F10 tumor-bearing mouse xenografts.

Materials and Methods

Materials

Paclitaxel (PTX) was purchased from Xi'an Haoxuan Biotechnology Co., Ltd. (Xi'an, China). Human serum

albumin was obtained from Yuanda Shuyang Pharmaceutical (Chengdu, China). Soybean oil was obtained from BASF (Ludwigshafen, Germany). 4′,6-Diamidino-2-phenylindole (DAPI) was purchased from Beyotime (Haimen, China). 1,1′-Dioctadecyl-3,3,3′,3′-tetramethylindodicarbocyanine perchlorate (Did) was provided by Sigma-Aldrich (St. Louis, MO, USA). All other reagents and chemicals used were of analytical grade.

Cell Culture and Animals

Cell Culture

Murine B16F10 melanoma cells, murine 4T1 breast cancer cells, human MCF-7 breast cancer cells, murine A549 lung cancer cells, dendritic cells (DC), and macrophage cells (RAW 264.7) were obtained from the Cell Bank of Chinese Academy of Sciences (CAS, Shanghai, China). All the cells were cultured in RPMI 1640 with 10% fetal bovine serum (Gibco, USA) and 1% penicillin/streptomycin. The cells were kept at 37°C in a humidified atmosphere containing 5% CO_2.

Animals

Female C57BL/6 mice (18–22 g) were purchased from Anhui Medical University (Hefei, China) and maintained under standard housing conditions. All animal protocols were approved by the Ethics Committee of Anhui Medical University (Laboratory animal-General guidelines for health monitoring T/CALAS 3–2017).

Preparation of Macrophage Membrane-Coated ANPs (RANPs)

To prepare RANPs, purified macrophage cell membranes were first collected. We used RAW 264.7 mouse macrophage cells as the model cell line. Membrane derivations were achieved by using a combination of hypotonic lysis, mechanical membrane fragmentation, and differential centrifugation to empty the harvested cells of their intracellular content. The collected membrane was then physically extruded through a 400 nm porous polycarbonate membrane to form macrophage cell membrane vesicles. Concurrently, albumin nanoparticles were prepared through a well-studied nanoprecipitation process.[36] In brief, human serum albumin (HSA) was dissolved in water. PTX and soybean oil were dissolved in dichloromethane and ethyl acetate. These solutions consisting of aqueous and organic phases were gently mixed and evaporated. To encapsulate the albumin nanoparticles within the macrophage cell membrane, the two components were then coextruded through a 200 nm porous polycarbonate membrane.

To determine the encapsulation efficiency, unentrapped PTX was separated by filtering through a 0.22 um membrane filter (We). The amount of PTX encapsulated within nanoparticles was determined by LC-MS/MS as previously reported.[37] An equal amount of micelles were dissolved in ethanol and subjected to LC-MS/MS analysis to determine the total amount of PTX (Wt). One milliliter of micelle was dried under vacuum to obtain the total weight of micelles (Wd). Encapsulation efficiency (EE) was calculated according to the equations as follows:

$$EE = We/Wt^{*}$$

Cellular Uptake and Internalization Pathways

B16F10 cells, 4T1 cells, MCF-7 cells, and A549 cells were cultured in 1 well plate (2×10^{5} cells per well) for 24 hrs. Did solution, ANPs/Did, and RANPs/Did at an equivalent dose of 5 μg/mL of Did were added into each well and co-incubated with B16F10 cells for 0.5 hr, 1 hr, and 2 hrs. At the given time points, the cells were washed three times with PBS. After centrifugation, cells were analyzed by flow cytometry (Beckman Coulter, USA). Then, the cells were fixed in 4% paraformaldehyde (20 min) and permeabilized in 0.5% Triton X-100 (20 min), which was followed by DAPI staining (5 min); the cells were then subjected to observation under confocal laser scanning microscope (CLSM) (Leica, Wetzlar, Germany).

To elucidate the internalization pathways of ANPs and RANPs in B16F10 cells, both nanoparticles were preincubated with selected endocytosis inhibitors, including amiloride (25 μM), chlorpromazine (20 μM), verapamil (6.5 mM) and colchicine (100 mM) for 1 hr at 37°C before the uptake study. Next, B16F10 cells were subjected to incubation at 37°C for another 1 hr after addition of ANPs/Did and RANPs/Did. The cells were then collected and subjected to flow cytometry analysis to determine the uptake efficiency.

Lysosomal Staining and Subcellular Distribution

To explore the subcellular localization behavior of nanoparticles, cell endosomes and lysosomes were labeled with LysoTracker Red (ThermoFisher Scientific, USA). Briefly, with the addition of ANPs/Coumarin 6 (C6) and RANPs/Coumarin 6 (C6) (5 μg/mL C6 per well), B16F10 cells were, respectively, incubated for 4 hrs and 24 hrs and were then

washed with PBS and stained with LysoTracker Red for 30 min prior to CLSM observation.

Cytotoxicity Assay

Viabilities of B16F10 cells after treatments with blank ANPs, blank RANPs, Taxol, ANPs/PTX, and RANPs/PTX were evaluated by standard MTT assay.[39] B16F10 cells were inoculated in 96-well plates (Corning, NY, USA) (1 × 104 cells per well). After 24 hrs, serum-free culture medium containing varying concentrations of blank ANPs, blank RANPs, Taxol, ANPs/PTX, and RANPs/PTX were incubated with cells for another 24 hrs. The mass concentration of albumin in blank ANPs and blank RANPs was kept the same as to the mass concentration of albumin in PTX-loaded ANPs and RANPs. Then, 20 μL of 5 mg/mL MTT solution was added into each well and incubated for 4 hrs in dark at 37°C. The medium was then discarded, and 200 μL of dimethyl sulfoxide was added to dissolve the formazan crystals in each well. The absorbance was measured at 570 nm on a microplate reader (Thermo Scientific, USA).

Tumor-Related Immune Cellular Uptake

Dendritic cells (DC) and RAW 264.7 cells were cultured in 12-well plates (2 × 10^5 cells per well) for 24 hrs. Did solution, ANPs/Did, and RANPs/Did at an equivalent dose of 5 μg/mL of Did were added into each well and coincubated with B16F10 cells for 1 hr, 2 hrs, and 4 hrs. At given time points, cells were washed three times with PBS. After centrifugation, the cells were analyzed by flow cytometry (Beckman Coulter, USA).

Cell Cycle and Cell Apoptosis and Necrosis

Cell-cycle distributions were assessed by propidium iodide (PI) staining as described in previous studies.[38] Briefly, B16F10 cells were seeded in six-well plates at 3 × 10^5 cells per well and incubated for 48 hrs at 37°C. Cells were then incubated with 2 mL of medium containing different concentrations of Taxol, ANPs/PTX, and RANPs/PTX for another 24 hrs. Subsequently, B16F10 cells were rinsed three times with PBS and fixed in cold 75% ethanol for 30 min at 4°C. After two PBS washes, the cells were incubated with 0.1 mL of 0.1% Triton X-100 for 15 min and 20 μg/mL ribonuclease A at 37°C for another 30 min; then, the cells were stained with 20 μg/mL PI at 4°C for another 30 min. All cell samples were then analyzed by flow cytometry (Cytomics FC500, Beckman Coulter, CA, USA).

B16F10 cells were seeded in six-well plates and cultured until reaching 40–50% confluence. Cells were then incubated with 2 mL of medium containing 1 mg/mL Taxol, ANPs/PTX, and RANPs/PTX for 12 hrs. Subsequently, the cells were rinsed with PBS twice and cultured with serum-free medium for another 48 hrs. The cells were then collected and stained with annexin V-FITC and propidium iodide (PI) according to the manufacturer's instructions (BD, USA). Stained cells were subjected to flow cytometry analysis to determine the percentages of apoptotic cells.

Biodistribution in Melanoma Xenograft Mice Model

B16F10 tumor-bearing female C57BL/6 mice were randomly divided into three groups (n = 3): Did solution, ANPs/Did, and RANPs/Did at an equivalent dose of 0.015 mg/kg, and saline was used as control. When solid tumors reached ~150 mm^3, mice were tail vein injected with Did solution, ANPs/Did, and RANPs/Did. After that, mice were subjected to anesthesia following i.p. injection of chloral hydrate, and ex vivo imaging was performed using IVIS® Spectrum (Caliper Life Sciences, PerkinElmer, USA) at 1 hr, 4 hrs, and 24 hrs post-injection of nanoparticles and Did solution. At given time points, mice were sacrificed, and their vital organs were excised for ex vivo fluorescence imaging.

In vivo Antitumor Efficacy

A total of 1 × 10^6 B16F10 cells were injected subcutaneously into the right flanks of female C57BL/6 mice. After one week, mice were randomly divided into four groups (n = 6), including saline, Taxol, ANPs/PTX, and RANPs/PTX. All PTX containing treatment groups were intravenously administered with the given formulation at an equivalent dose of 1 mg/kg PTX. Ten days after tumor inoculation, all treatments were administered via tail vein injection once every other day four consecutive times. The tumor diameters were measured every other day. Tumor volume (V) was then calculated using the following formula: volume = (L × W^2)/2. Length (L) and width (W) represent the longest and shortest diameter, respectively. To evaluate proliferation, apoptosis, and neovascularization, immunohistochemical staining was performed on paraffin-embedded tumor sections.

Statistical Analysis

All data were presented as the means ± standard deviations (S.D.). For comparison among multiple groups, one-way ANOVA was performed, followed by a Tukey post hoc

analysis. A p-value of less than 0.05 was considered statistically significant.

Results

Characterization of ANPs and RANPS

The hydrodynamic diameter of the membrane was less than 300 nm as measured by dynamic light scanning, and ANPs displayed an average size distribution of 138.7 ± 3.5 nm (Table 1). Upon fusion of the membrane vesicles with the albumin nanoparticles, the final average size of RANPs was 188.7 ± 4.8 nm (Figure 1C), which is between the size of ANPs and the membranes. For the surface charge, RANPs showed an average charge of −10.5 mV. Zeta potential measurements also suggested successful coating. Specifically, after being coated, the surface charge of the albumin cores increased to approximately the level of the membrane vesicles (Table 1). The membrane coating around the polymer nucleus was observed by transmission electron microscopy (TEM). RANPs were spherical and showed a core-shell structure using negative staining (Figure 1C). On the basis of some previous studies on membrane-coated nanoparticles,[39] it was expected that the coating on RANPs would transmigrate faithfully to the surface of the nanoparticles as a membrane bilayer, resulting in the right outer conformation allowing the membrane to maintain its ability. Additionally, the encapsulation efficiencies of ANPs/PTX and RANPS/PTX were found to be 93.5 ± 2.1% and 83.4 ± 2.2%, respectively, demonstrating that the formulations can further be used in the antitumor study in vitro and in vivo.

Cellular Uptake Efficiency, Internalization Pathways, and Intracellular Distribution

To investigate the cellular uptake efficiency of ANPs and RANPs, a near-infrared fluorescent probe (Did) was used instead of PTX. Did-loaded nanoparticles such as ANPs/Did and RANPs/Did were fabricated following the same method of PTX-loaded nanoparticles as described in the method section. To evaluate whether RANPs could be specifically taken up by tumor cells, we chose four kinds of tumor cells (4T1, A549, MCF-7, and B16F10 cells). According to the flow cytometry results, both ANPs/Did and RANPs/Did showed time-dependent increases in the fluorescence intensity in four tumor cells (Figure 2). At all given time points, RANPs/Did showed significantly higher uptake efficiencies ($p < 0.05$) compared to ANPs/Did in tumor cells. Additionally, in B16F10, the uptake efficiency of RANPS/Did was 3.41 times higher than that of cells treated with ANPs/Did at 0.5 hr, 4.3 times higher at 1 hr, and 5.88 times higher at 2 hrs, respectively ($p < 0.05$). Consistent with quantitative flow results, CLSM images showed a greatly enhanced intracellular distribution of Did fluorescence in the RANPs group, and Did fluorescence intensity increased over time; in the ANPs/Did group, the fluorescence intensity remained much weaker (Figure 3A).

To elucidate the internalization pathways of RANPs/Did in B16F10 cells, classic endocytosis inhibitors were selected.[40] The uptake efficiencies of ANPs/Did and RANPs/Did at 4°C were much lower than that at 37°C ($p < 0.05$), indicating that the internalization processes of both ANPs and RANPs were energy-driven. Additionally, both chlorpromazine and verapamil treated groups exhibited significant uptake reduction compared to the control ($p < 0.05$), while other endocytosis inhibitors such as amiloride did not affect the uptake efficiency, which suggested that the endocytosis of both nanoparticles was mainly mediated by clathrin-dependent, caveolae-independent and macropinocytosis-independent pathways (Figure 3B and C).

Next, the intracellular distribution profiles of ANPs and RANPs in B16F10 cells were studied using CLSM. In the following study, coumarin 6 (C6) was selected as the model compound to demonstrate the intracellular distribution pattern of nanoparticles. LysoTracker Red was used to label lysosomes in B16F10 cells. At given time points, both ANPs and RANPS showed internalization in B16F10 cells (Figure 4). Notably, RANPs showed more enhanced fluorescence intensity than ANPs at 2 hrs (Figure 4B), which is consistent with the flow cytometry results. At 24 hrs, both ANPs and RANPS showed extensive intracellular distributions in the cytoplasm (Figure 4); the green and red fluorescence overlapped significantly, suggesting a lysosomal pathway after internalization. Regarding the internalization behavior and intracellular distribution pattern, no obvious differences were observed between ANPs and RANPs.

Table 1 Characterization of ANPs, Membrane, and RANPs. Data Represent Mean ± SD (n = 3)

	Size (nm)	Zeta Potential (mV)	EE (%)
ANPs	138.7 ± 3.5	−15.7 ± 2.5	93.5 ± 2.1
Membrane	208.5 ± 6.1	−9.6 ± 1.1	—
RANPs	188.7 ± 4.8	−10.5 ± 2.2	83.4 ± 2.2

Immune Cell Uptake Efficiency in Tumor Microenvironment

It is now widely believed that the immune system is also capable of constantly checking and removing precancerous

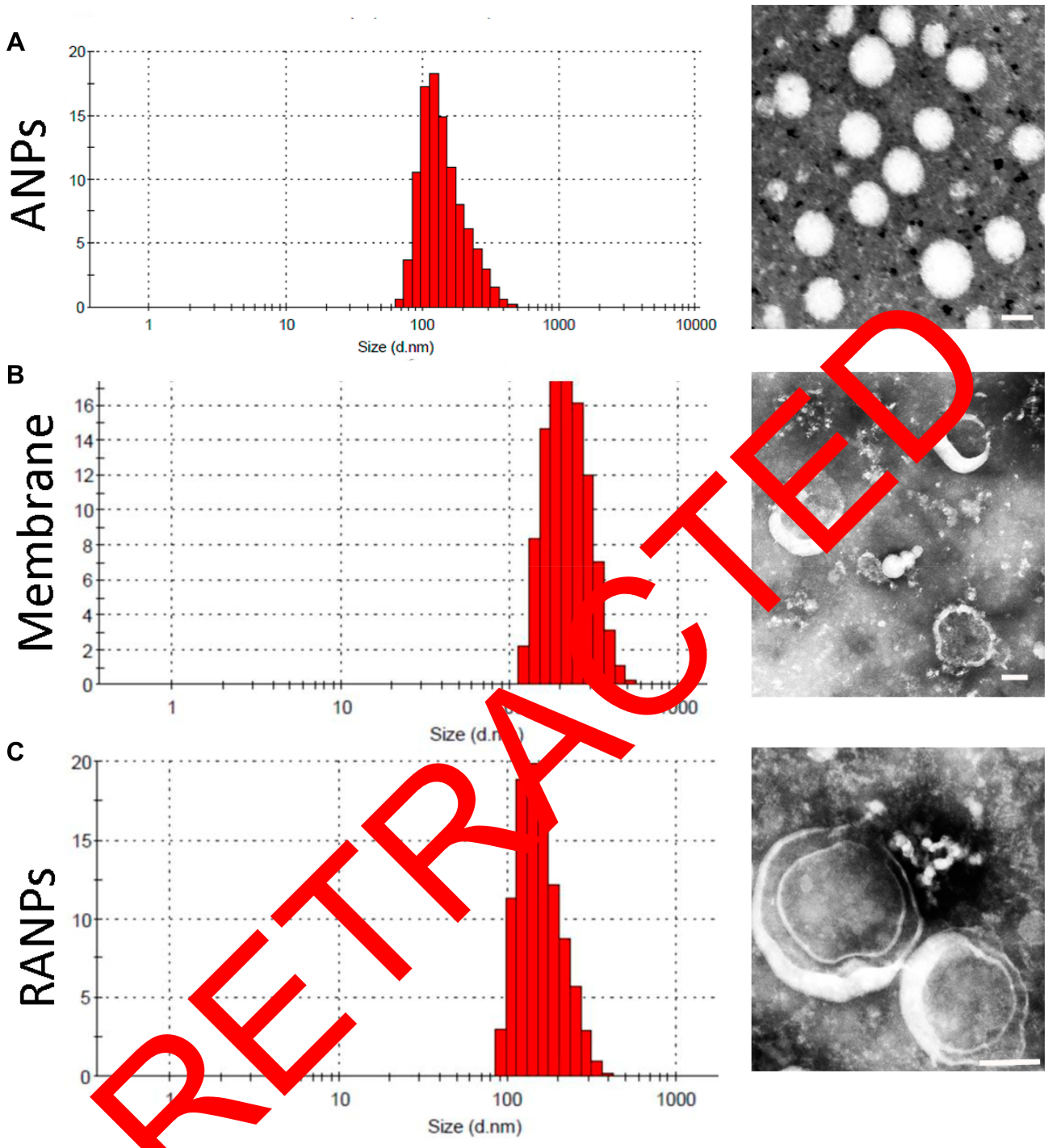

Figure 1 Size distribution and morphology of nanoparticles: Dynamic light scattering (DLS) size measurement and TEM image of (**A**) ANPs, (**B**) membranes, and (**C**) RANPs. Scale bar represents 100 nm.

cells to prevent the development of melanoma.[41] DC cells and RAW264.7 cells, as two important immune cell types in the tumor microenvironment, were chosen to investigate the uptake efficiency of RANPs. According to flow cytometry results, both ANPs/Did and RANPs/Did showed time-dependent increases in the fluorescence intensity in the two types of immune cells. At all given time points, RANPs/Did showed significantly higher uptake efficiencies ($p < 0.05$) compared to ANPs/Did in tumor cells (Figure 5). The results showed that the preparation could be specifically ingested by immune cells, thereby may affect tumor growth at the immune level.

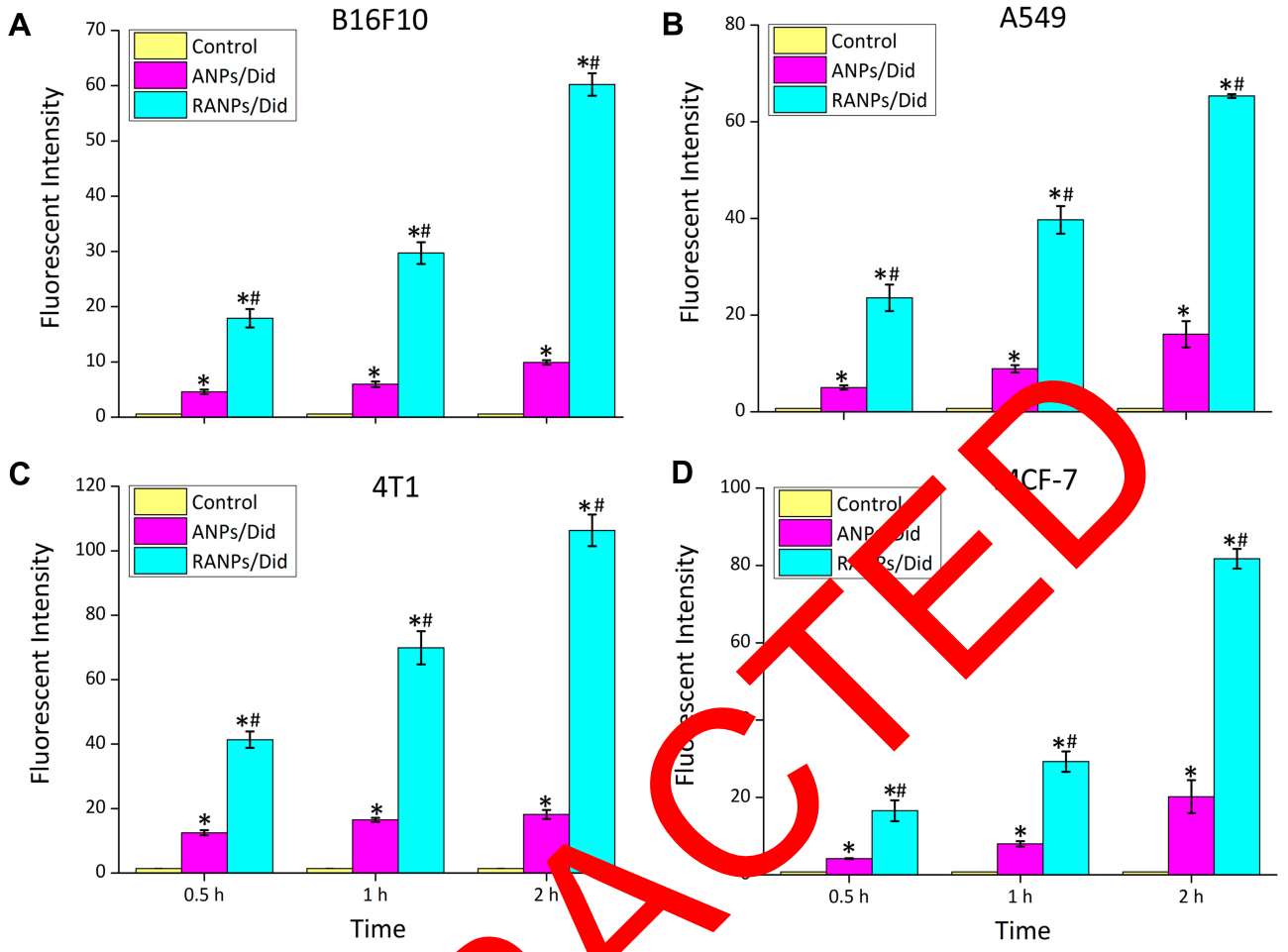

Figure 2 Time-dependent cellular uptake of ANPs/Did and RANPs/Did after incubation with B16F10 (**A**), A549 (**B**), 4T1 (**C**)and MCF-7 cells (**D**) for 0.5 hr, 1 hr, and 2 hrs as determined by flow cytometry analysis. Data represent means ± SD (n = 3). *p < 0.05 vs control. #p < 0.05 vs ANPs/Did.

Cytotoxicity

First, cell viability of blank ANPs and blank RANPS against B16F10 cells was evaluated by standard MTT assay. Both blank NPs and RANPS displayed no obvious cytotoxicity against B16F10 cells at all concentrations under investigation (Figure 6), indicating nanoparticle vehicles were of minimal cytotoxicity against B16F10 cells. For each concentration under investigation, both ANPs/PTX and ARNPs/PTX showed much higher inhibitory effect compared to PTX solution in B16F10 cells after 24 hrs of treatment. Moreover, RANPs/PTX showed greater cytotoxicity as compared to ANPs/PTX (Figure 6).

Cell Cycle and Cell Apoptosis

PTX has been proven to impact the cell cycle by arresting cells in the G2/M phase.[42] To estimate the in vitro antimitotic effect of ANPs and RANPs at the cellular level, cell cycle analysis was performed, and the results are presented in Figure 7. Compared to Taxol, ANPs/PTX and RANPs/PTX arrested fewer cell populations in the G0/G1 phase ($p < 0.05$) and more cells in the G2/M phase ($p < 0.05$). Furthermore, ANPs/PTX-treated groups showed significantly more cell populations in the sub-G1 phase than that in the Taxol-treated group ($p < 0.05$). Because the sub-G1 phase is a characteristic hypodiploid DNA content peak representing apoptotic and necrotic cell populations, more cells in the sub-G1 phase in the RANPs/PTX-treated group may indicate more cells likely undergo apoptosis. Further, RANPs/PTX could induce more cell apoptosis, which is likely due to the coating of the macrophage cell membrane.

Biodistribution of RANPs/Did in Melanoma Xenograft Model

To gain insight into biodistribution of RANPs, ex vivo fluorescence imaging was performed in B16F10 bearing C57BL/6 mice at 1 hr, 4 hrs, and 24 hrs after systemic administration of ANPs/Did and RANPs/Did. The biodistribution of the

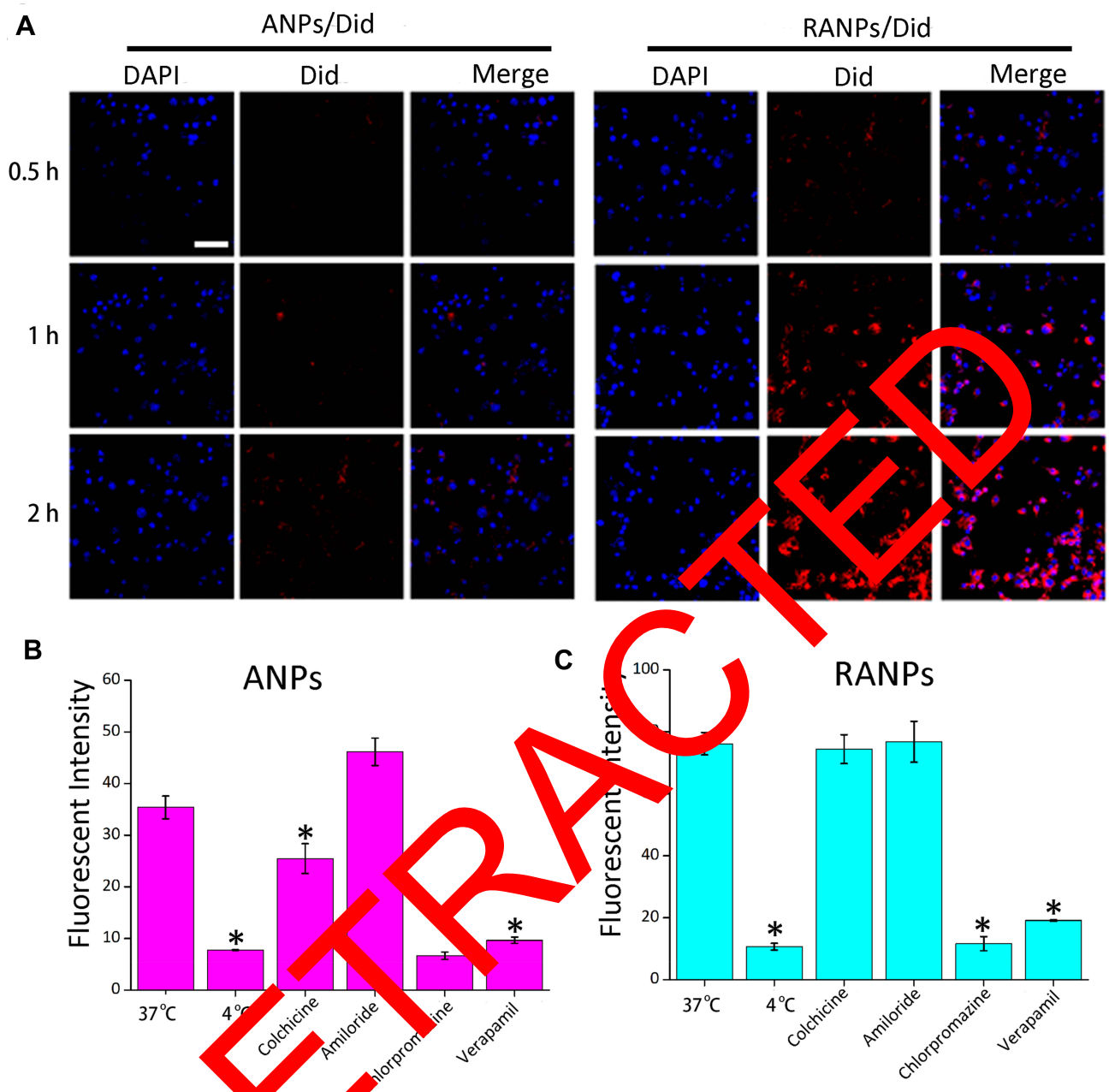

Figure 3 (**A**) Representative confocal laser scanning microscopy images of B16F10 cells after incubation with ANPs/Did and RANPS/Did for 0.5 hr, 1 hr, and 2 hrs. DAPI stains for cell nuclei (blue) and represents ANPs or RANPs (red). Scale bar represents 100 μm. (**B, C**) Internalization pathways of ANPs and RANPs in B16F10 cells. B16F10 cells were preincubated under various conditions including 4°C, chlorpromazine, verapamil, amiloride, and colchicine. Data represent means ± SD (n = 3). *$p < 0.05$ vs 37°C.

nanoparticles in major organs and tumors at the given time points is shown in Figure 8. Among two treatment groups, dramatic accumulations of fluorescence signals in the liver and kidney were observed (Figure 8A). Regarding Did distribution in the tumor tissues, RANPs/Did group displayed remarkably higher accumulation at the tumor site than ANPs/Did group after 24 hrs, indicating RANPs have greater tumor-specific distribution (Figure 8C). Meanwhile, RANPs/Did also displayed the highest fluorescence intensity in blood after 24 hrs (Figure 8B), suggesting a prolonged circulation of RANPs as compared to ANPs.

In vivo Antitumor Efficacy and Systemic Toxicity

To explore the antitumor efficacy of RANPs/PTX in vivo, melanoma xenograft models were established in C57BL/6 mice. As shown in Figure 9, the RANPs/PTX-treated group showed remarkably better treatment effects than the saline

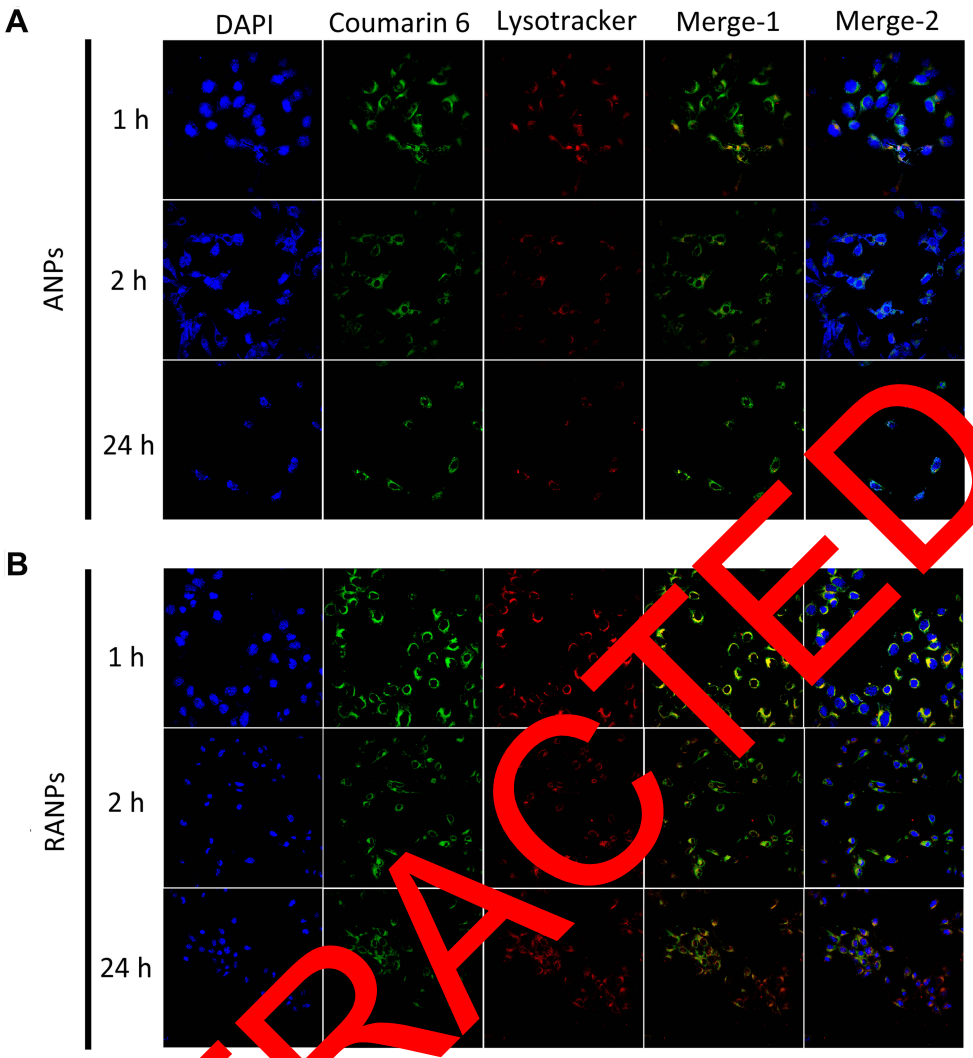

Figure 4 Representative confocal images of 5F10 cells incubated with coumarin 6-loaded nanoparticles (ANPs/C6 (**A**) and RANPs/C6 (**B**)) and LysoTracker Red for 1 hr, 2 hrs, and 24 hrs. Scale bar represents 2 μm.

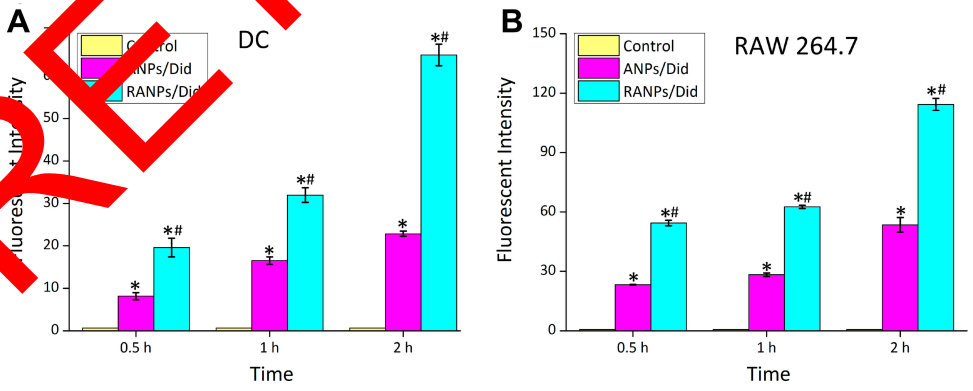

Figure 5 Time-dependent cellular uptake of ANPs/Did and RANPs/Did after incubation with DCs (**A**) and RAW 264.7 cells (**B**) for 0.5 hr, 1 hr, and 2 hrs as determined by flow cytometry analysis. Data represent means ± SD (n = 3). *$p < 0.05$ vs control. #$p < 0.05$ vs ANPs/Dids.

control, Taxol, and ANPs/PTX-treated group, presenting the smallest tumor volumes among treatment groups at all given time points ($p < 0.05$) (Figure 9A and B). Although the tumor inhibition rate of ANPs/PTX and RANPs/PTX was distinctly higher than that of the Taxol-treated group, the RANPs/PTX-treated group showed the highest tumor inhibition rate

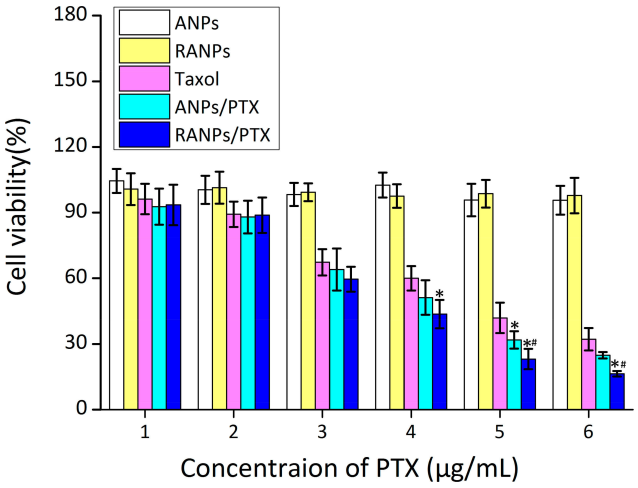

Figure 6 Cell viability of B16F10 after 24 hrs of treatment of blank ANPs, blank RANPs, Taxol, ANPs/PTX, and RANPs/PTX with varying concentrations. Data represent mean ± SD (n = 3). *$p < 0.05$ vs control. #$p < 0.05$ vs ANPs/Did.

among all treatment groups (Figure 9D). On the other hand, the weight changes and morphology of the different treatment groups were not significant (Figure 9C and E), revealing reduced systemic toxicity of the nanoparticles.

Discussion

With increasing understanding of the biomimetic scienc nanoscale delivery systems coated with plasma membranes have attracted extensive attention in the past few ca Thus far, nanoparticles coated with cancer cell mem anes, b erial membranes, red blood cell membranes, le kocy m branes, and macrophage membranes have bee reported f the delivery of small molecule drugs, antib ies, d vaccines. rious technologies have been develoed to fabri te plasma membrane-coated nanoparticles or example, the s assembly of leukocyte membrane- ted na particles was driven by electrostatic and hydrophobic interactions between the negatively charged proteo-lipid patches and the positively charged nanoparticle surface under continuous rotation, while emtansine liposomes coated with macrophage membranes were fabricated by a direct extrusion method. These "biomimetic camouflage" strategies utilize the function of plasma membranes to help nanoparticles escape from the immune system and cross the biological barriers. Moreover, nanoparticles coated with plasma membranes possess cell-like properties and behaviors, thus increasing the affinity toward target cells and cell membrane interactions.

In this study, we successfull prepared TX-loaded albumin nanoparticles coated with acrophage membranes to achieve targeted therapy f melano a in vi . PTX has demonstrated potent tumor in ibitory ects against a variety of tumor cells. or ample, PTX could successfully suppress A 49 cance growth Additionally, PTX can inhibit ce cell invasi via suppression of NF-κB-mediated matrix talloproteinase-9 expression.[44,45]

In our study, co ared to ANPs/PTX without a acrophage membrane coating, RANPs/PTX showed imp ved antitu r efficacy both in vitro and in vivo (Figur 6). Firs the cell uptake efficiency of RANPs in 16F10 cells and three other tumor cells was significantly in reased when coated with macrophage membranes compared to that of ANPs ($p < 0.05$). However, coating nanoparticles with macrophage membranes did not change the overall internalization pathway and the intracellular distribution pattern of the nanoparticles (Figure 4). This result indicates that the presence of macrophage membranes effectively increased the internalization efficiency of nanoparticles in B16F10 cells without changing its internalization pathway. The increased cell uptake efficiency in tumor cells might be due to the

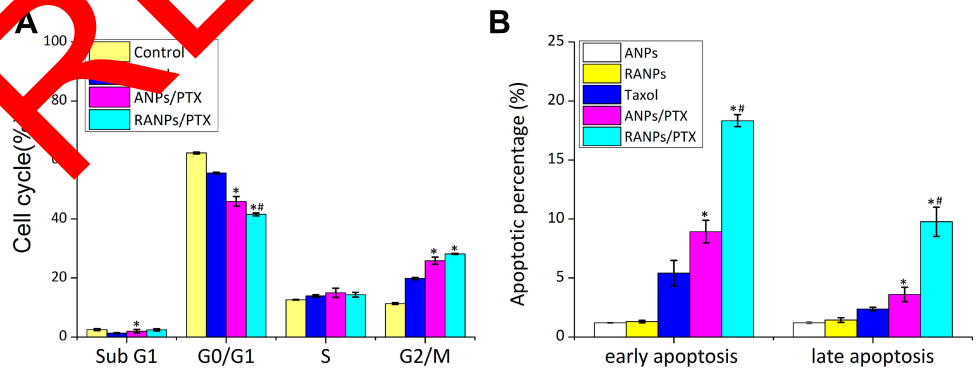

Figure 7 (**A**) Cell cycle distributions of B16F10 cells after various treatments with equivalent doses of PTX. (**B**) The apoptotic cell percentages of B16F10 cells after various treatments of blank ANPs, blank RANPs, Taxol, ANPs/PTX, and RANPs/PTX. An equivalent dose of 1 μg/mL PTX was used, and the concentrations of blank nanoparticles were maintained the same as the PTX-loaded nanoparticles. Data represent means ± SD (n = 3). *$p < 0.05$ vs Taxol, #$p < 0.05$ vs ANPs/PTX.

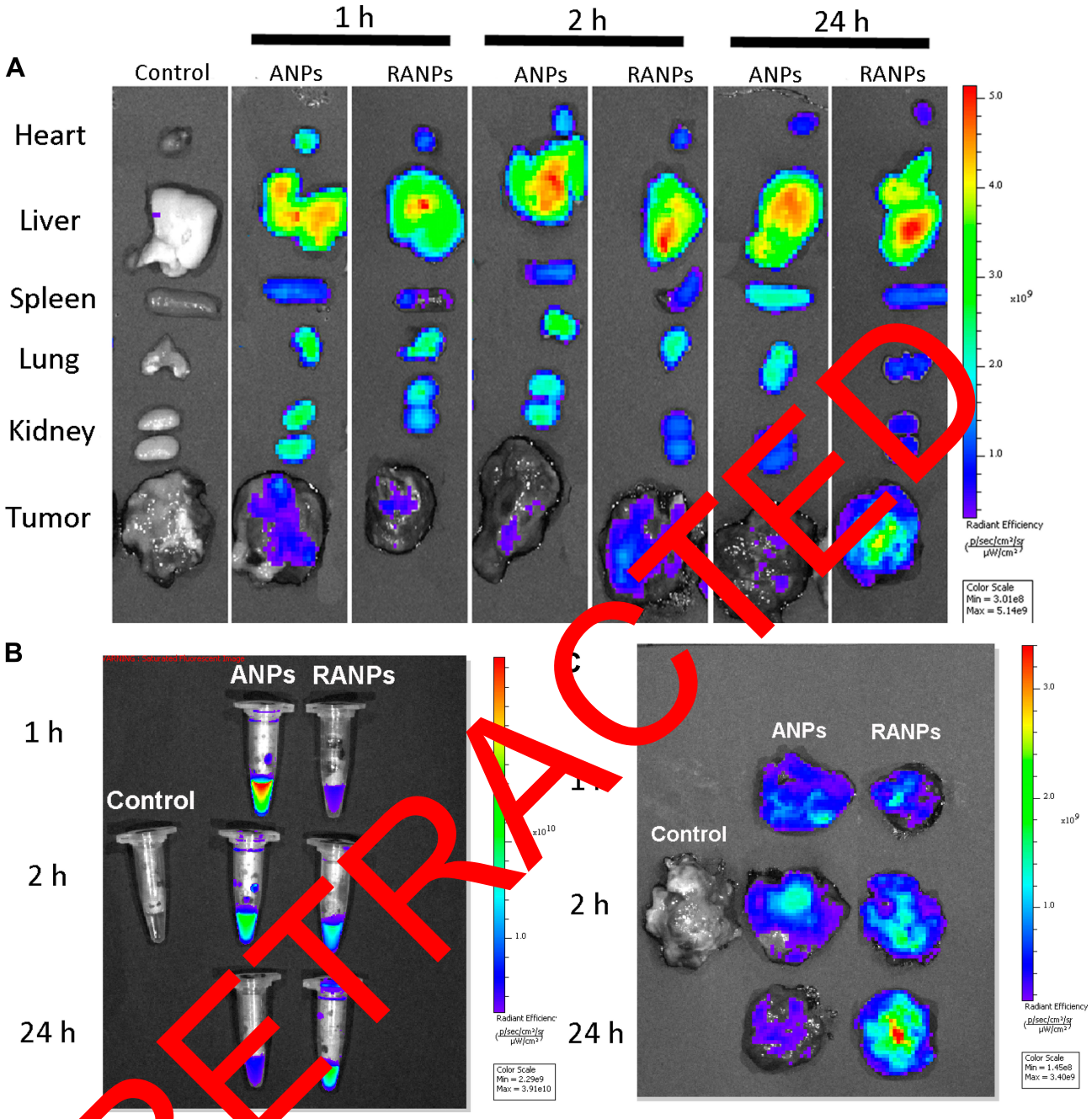

Figure 8 distributi of Did-loaded nanoparticles in melanoma xenograft mice. Did-loaded nanoparticles were administered via tail vein injection at an equivalent dose of 0.01 /k (**A**) Ex vivo fluorescence imaging of major organs at 1 hr, 2 hrs, and 24 hrs after injection. (**B**) Ex vivo imaging of blood at given time points. (**C**) Ex vivo imaging of excis umors at the given time points.

enhanced affinity between RANPs and the tumor cell membrane. The results of uptake of DC and RAW cells also suggest that RANPs may also be involved in tumor immunotherapy due to the specific proteins on the surface of RANPs. Albumin-based cancer drug delivery systems have shown prolonged blood circulation time and high drug accumulation in tumors.[46,47] However, albumin-based nanoscale delivery systems have low stability in blood circulation, resulting in premature nanoparticle dissociation and early drug release before reaching the tumor target.[48] The biodistribution study using tumor-bearing mice demonstrated that RANPs had relatively longer retention in circulation and selective accumulation in the tumor sites (Figure 8). Nanoparticles coated with plasma membranes can be more easily taken up by tumor cells and showed enhanced internalization efficiency in tumor cells compared to nanoparticles without plasma membrane

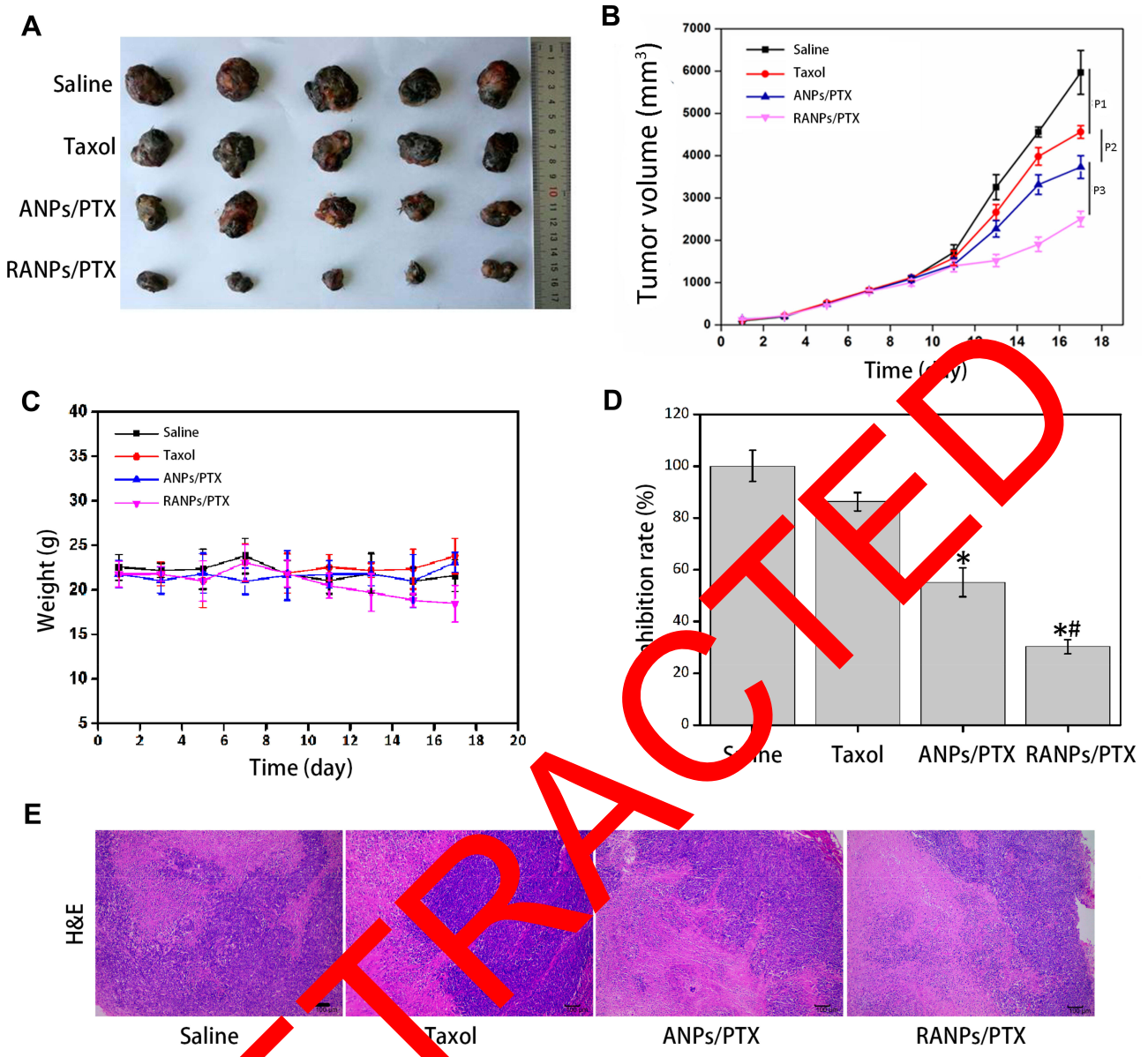

Figure 9 The antitumor efficacy of PTX-loaded nanoparticles in C57BL/6 mice bearing B16F10 melanoma xenografts. (**A**) Images of excised B16F10 tumors collected from each treatment. (**B**) Average tumor volume after treatment over the investigative period (n = 5). *$p < 0.05$ vs Taxol, #$p < 0.05$ vs ANPs/PTX. (**C**) Bodyweight variations of mice bearing B16F10 melanoma xenografts after each treatment over time. (**D**) Tumor inhibition rate after treatment. (**E**) Morphology of RANPs/PTX-treated groups. Sections were isolated and stained with hematoxylin and eosin (H&E) for histopathological analysis. Scale bar represents 100 μm. Data represent means ± SD (n = 5).

coatings, which were similar to RBC-membrane-coated nanoparticles.[49] These results were also consistent with in vitro cytotoxicity and cellular uptake results, demonstrating that nanoparticles coated with macrophage membranes showed enhanced efficacy both in vitro and in vivo.

In systemic circulation, macrophages recognize nanoparticles coated with macrophage membranes and consider them as a part of the body, thereby escaping clearance by the immune system. Then, the granulocyte colony-stimulating factor in the inflammatory microenvironment of the tumor releases a signal to gather nanoparticles coated with macrophage membranes because of the receptor–ligand interactions.[50] Pharmacodynamic studies demonstrated the antitumor efficacy of RANPs/PTX in vivo. These results revealed that RANPs could be targeted to cancer cells. The targeting ability of nanoparticles coated with macrophage membranes is extremely likely because the macrophage membrane coated on albumin nanoparticles may retain inflammation-associated proteins, which may facilitate the accumulation of nanoparticles in the tumor inflammatory microenvironment.[51,52]

Conclusion

Overall, albumin-based nanoscale delivery systems coated with macrophage plasma membranes remain a highly promising delivery system with a prolonged circulation profile and without premature drug release; further, these systems offer improved tumor targetability that can be applied to various drug compounds with varying physicochemical properties. Specifically, the presence of macrophage membranes on the nanoparticle surface significantly enhanced the cellular uptake efficiency in B16F10 cells without changing their major internalization pathways. Additionally, the presence of macrophage membranes induced more specific accumulation at the tumor site and stronger antitumor efficacy. Taken together, albumin nanoparticles coated with macrophage membranes present a neat and efficient strategy to achieve targeted melanoma chemotherapy.

Acknowledgment

Authors are very grateful for the financial support from Anhui Province Natural Science Foundation (No.1808085MH235).

Disclosure

The authors report no conflicts of interest in this wo[illegible].

References

1. Balch CM, Soong SJ, Gershenwald JE, et a[illegible] Prognost[illegible] ana[illegible] lysis of 17,600 melanoma patients: vali[illegible]tion [illegible] American Joint Committee on cancer melanoma [illegible]ging syst[illegible] *J Clin Oncol*. 2001;19(19):3622–3634. doi:10.12[illegible]JCO.2001.19.1[illegible]22
2. Chen X, Yang M, Hao W[illegible]t al. [illegible]fferentiation-inducing and anti-proliferative activities [illegible]f isoliquiritig[illegible]in and all-trans-retinoic acid on B16F0 melanom[illegible] cells: mechanisms [illegible]ofiling by RNA-seq. *Gene*. 2016;592(1):86[illegible]8. doi:10.1016/j.gene.2016.07.052
3. Hahne M, Rimoldi[illegible] Schröte[illegible]M, et al. Melanoma cells express fas ligand: implications [illegible]t[illegible]r immun[illegible]escape. *Science*. 1996;274 (5291):1363[illegible] doi:10[illegible]26/scien[illegible]274.5291.1363
4. Meier F, [illegible]sch S, [illegible]sithiotak[illegible]K[illegible]al. Combined targeting of MAPK and AK[illegible] signallin[illegible] pathways [illegible]a promising strategy for melanoma treatme[illegible] *Br*[illegible] 2007;156(6):1204–1213. doi:10.1111/j.1365-21[illegible]07.07821.x
5. Chezal JM, [illegible]on J, Labarre P, et al. Evaluation of radiolabeled (hetero)aromatic[illegible]nalogues of N-(2-diethylaminoethyl)-4-iodobenzamide for imaging and targeted radionuclide therapy of melanoma. *J Med Chem*. 2008;51(11):3133–3144. doi:10.1021/jm701424g
6. Nestle FO, Gilliet M, Alijagic S, et al. Vaccination of melanoma patients with peptide-pulsed dendritic cells: 047. *Melanoma Res*. 1997;7 (Supplement 1):S14. doi:10.1097/00008390-199706001-00047
7. Coit DG, Thompson JA, Algazi A, et al. Melanoma, version 2.2016. *J Natl Compr Canc Netw*. 2016;14(4):450-+. doi:10.6004/jnccn.2016.0051
8. Yu M, Xue Y, Ma PX, Mao C, Lei B. Intrinsic ultrahigh drug/miRNA loading capacity of biodegradable bioactive glass nanoparticles towards highly efficient pharmaceutical delivery. *ACS Appl Mater Interfaces*. 2017;9(10):8460–8470. doi:10.1021/acsami.6b13874
9. Wang Q, Zhang X, Liao H, et al. Multifunctional shell-core nanoparticles for treatment of multidrug resistance hepatocellular carcinoma. *Adv Funct Mater*. 2018;28(14):1706124. doi:10.1002/adfm.v28.14
10. Sengupta S, Eavarone D, Capila I, et al. Temporal targeting of tumour cells and neovasculature with a nanoscale delivery system. *Nature*. 2005;436(7050):568–572. doi:10.1038/nature03794
11. Cao X, Luo J, Gong T, Zhang Z, Sun X, Fu Y. Coencapsulated doxorubicin and bromotetrandrine lipid nanoemulsions in reversing multidrug resistance in breast cancer in vitro and in vivo. *Mol Pharm*. 2015;12(1):274–286. doi:10.1021/mp500637b
12. Mitra S, Gaur U, Ghosh PC, Maitra AN. Tumour targeted delivery of encapsulated dextran-doxorubicin conjugate using chitosan nanoparticles as carrier. *J Control Release*. 2001;74(1–3):317–323. doi:10.1016/S0168-3659(01)00342-X
13. Ruff J, Hüwel S, Kogan MJ, Simon U[illegible]HJ. The effects of gold nanoparticles functionalized with [illegible]myloid s[illegible]ific peptides on an in vitro model of blood-br[illegible] barrier. *Nan[illegible]ed-Nanotechnol*. 2017;13(5):1645. doi:10.1016/j.na[illegible]2017.02.013
14. Niu F, Yan J, Ma B, et al. [illegible]nthanide[illegible]ped nano[illegible]ticles conjugated with an anti-CD33 an[illegible]ody and a p53[illegible]tiva[illegible]g peptide for acute myeloid leukemia t[illegible]rapy. *Bio[illegible]terials*. 2[illegible],167:132. doi:10.1016/j.biomaterials.2018.0[illegible]025
15. Paciotti GF, L[illegible]ngston D[illegible]Tamarkin [illegible]Colloidal gold nanoparticles: a novel [illegible]noparticle p[illegible]form[illegible]or developing multifunctional tumor-[illegible]gete[illegible]drug delivery [illegible]tors. *Drug Develop Res*. 2006;67 (1):47–54. doi:[illegible]002/(ISSN)1098-2299
16. C[illegible]Y, Bathula SR[illegible]ang Q, Huang L. Targeted nanoparticles deliver siRNA to melanoma. *[illegible]Invest Dermatol*. 2010;130(12):2790–2798. doi:10.1038/jid.2010.222
17. Cao H, Da[illegible]Z, He X, et al. Liposomes coated with isolated macrophage[illegible]membrane can target lung metastasis of breast [illegible]ncer. *A[illegible]Nano*. 2016;10(8):7738–7748. doi:10.1021/acsnano.6b03148
18. Sun H, Su J, Meng Q, et al. Cancer-cell-biomimetic nanoparticles for targeted therapy of homotypic tumors. *Adv Mater*. 2016;28 (43):9581–9588. doi:10.1002/adma.201602173
19. Anselmo AC, Mitragotri S. Cell-mediated delivery of nanoparticles: taking advantage of circulatory cells to target nanoparticles. *J Control Release*. 2014;190:531–541. doi:10.1016/j.jconrel.2014.03.050
20. Cao H, Dan Z, He X, et al. Liposomes coated with isolated macrophage membrane can target lung metastasis of breast cancer. *ACS Nano*. 2016;10(8):7738. doi:10.1021/acsnano.6b03148
21. Fang RH, Hu CM, Luk BT, et al. Cancer cell membrane-coated nanoparticles for anticancer vaccination and drug delivery. *Nano Lett*. 2014;14(4):2181–2188. doi:10.1021/nl500618u
22. Dehaini D, Wei X, Fang RH, et al. Erythrocyte-platelet hybrid membrane coating for enhanced nanoparticle functionalization. *Adv Mater*. 2017;29(16):1606209. doi:10.1002/adma.201606209
23. Bunt SK, Yang L, Sinha P, Clements VK, Leips J, Ostrand-Rosenberg S. Reduced inflammation in the tumor microenvironment delays the accumulation of myeloid-derived suppressor cells and limits tumor progression. *Cancer Res*. 2007;67(20):10019. doi:10.1158/0008-5472.CAN-07-2354
24. Hazeldine J, Harris P, Chapple IL, et al. Impaired neutrophil extracellular trap formation: a novel defect in the innate immune system of aged individuals. *Aging Cell*. 2014;13(4):690. doi:10.1111/acel.12222
25. Kumar V, Sharma A. Neutrophils: cinderella of innate immune system. *Int Immunopharmacol*. 2010;10(11):1325–1334. doi:10.1016/j.intimp.2010.08.012
26. Kang T, Zhu Q, Wei D, et al. Nanoparticles coated with neutrophil membranes can effectively treat cancer metastasis. *ACS Nano*. 2017;11(2):1397. doi:10.1021/acsnano.6b06477
27. Xue J, Zhao Z, Zhang L, et al. Neutrophil-mediated anticancer drug delivery for suppression of postoperative malignant glioma recurrence. *Nat Nanotechnol*. 2017;12(7):692. doi:10.1038/nnano.2017.54

28. Le QT, Byeon HJ, Lee C, et al. Doxorubicin-bound albumin nanoparticles containing a TRAIL protein for targeted treatment of colon cancer. *Pharm Res*. 2016;33(3):615–626. doi:10.1007/s11095-015-1814-z
29. Kim B, Seo B, Park S, et al. Albumin nanoparticles with synergistic antitumor efficacy against metastatic lung cancers. *Colloids Surf B Biointerfaces*. 2017;158:157. doi:10.1016/j.colsurfb.2017.06.039
30. Kratz F. Albumin as a drug carrier: design of prodrugs, drug conjugates and nanoparticles. *J Control Release*. 2008;132(3):171–183. doi:10.1016/j.jconrel.2008.05.010
31. Taheri A, Dinarvand R, Ahadi F, Khorramizadeh MR, Atyabi F. The in vivo antitumor activity of LHRH targeted methotrexate-human serum albumin nanoparticles in 4T1 tumor-bearing Balb/c mice. *Int J Pharm*. 2012;431(1–2):183–189. doi:10.1016/j.ijpharm.2012.04.033
32. Maeda H, Wu J, Sawa T, Matsumura J, Hori K. Tumor vascular permeability and the EPR effect in macromolecular therapeutics: a review. *J Control Release*. 2000;65(1–2):271–284. doi:10.1016/S0168-3659(99)00248-5
33. Joos G, Schallier D, Pinson P, Sterckx M, Meerbeeck JPV. Paclitaxel (PTX) as second line treatment in patients (pts) with small cell lung cancer (SCLC) refractory to carboplatin - etoposide: a multicenter Phase II study. *J Clin Oncol*. 2004;22(14_suppl):7211. doi:10.1200/jco.2004.22.14_suppl.7211
34. Liu Z, Tong Y, Liu Y, et al. Effects of suberoylanilide hydroxamic acid (SAHA) combined with paclitaxel (PTX) on paclitaxel-resistant ovarian cancer cells and insights into the underlying mechanisms. *Cancer Cell Int*. 2014;14(1):139.
35. Wu J, Liu Y, Tang Y, et al. Synergistic chemo–photothermal therapy of breast cancer by mesenchymal stem cell-encapsulated yolk–shell GNR@HPMO-PTX nanospheres. *ACS Appl Mater Interfaces*. 2016;8(28):17927–17935.
36. Guo L, Luo S, Du Z, et al. Targeted delivery of celastrol to mesangial cells is effective against mesangioproliferative glomerulonephritis. *Nat Commun*. 2017;8(1):878. doi:10.1038/s41467-017-00834-8
37. Suzuki T, Beuzenberg V, Mackenzie L, Quilliam MA. Liquid chr matography–mass spectrometry of spiroketal stereoisomers of pecte notoxins and the analysis of novel pectenotoxin isomers i the toxic dinoflagellate dinophysis acuta from New Zealand. *J hromatogr A*. 2003;992(1–2):141–150. doi:10.1016/S0021-9673( )00324-
38. Cao X, Hu Y, Luo S, et al. Neutrophil-mimicki therape particles for targeted chemotherapy of pa creatic oma. *Acta Pharm Sin B*. 2019;9(3):575–589. doi:10 016/j.apsb.2 8.12.009
39. Gao W, Zhang L. Engineering re d-cell-membr -coated nanoparticles for broad biomedica applica s. *AIChE J*. 2015;61(3):738–746. doi:10.1002/aic.v6 3
40. Ward ME, Murray A. Contr mechanisms goveri the infectivity of Chlamydia tracho s for L La cells: mechanisms of endocytosis. *J Gen M biol*. 1 4;130(7):1765–1780. doi:10.1099/00221287-130-7-1765
41. Wang J, Li D, Cang H, Guo B. Crosstalk between cancer and immune cells: role of tumor-associated macrophages in the tumor microenvironment. *Cancer Med*. 2019;8(10):10. doi:10.1002/cam4.v8.10
42. Shin JY, Park JK, Kuh HJ, Kang JH. Additive cytotoxicities, apoptosis and cell cycle changes induced by combination treatment of celecoxib and paclitaxel in A549 NSCLC cell line. *Cancer Res*. 2004;64:1228.
43. Jiang J, Liu Y, Wu C, et al. Development of drug-loaded chitosan hollow nanoparticles for delivery of paclitaxel to human lung cancer A549 cells. *Drug Dev Ind Pharm*.2017;43(8):1304–1313.
44. Zhang Y, Wang Y, Xue J. Paclitaxel inhibits breast cancer metastasis via suppression of Aurora kinase-mediated cofilin-1 activity. *Exp Ther Med*. 2018;15(2):1269–1276. doi:10.3892/etm.2017.5588
45. Jiang Z, Zhang SJ, Chen B, Gao F. Pa axel inhib proliferation and matrix metalloproteinases (MM –2, MMP −9) pression in ovarian cancer HO8910 cells. *Chinese Pharm Anal s*. 2002;22(6):458–461.
46. Elzoghby AO, Samy WM lgindy NA. A mi based nanoparticles as potential c rolled r ase drug elivery systems. *J Control Release*. 20 157 168–182 doi:10.1016/j.jconrel.2011.07.031
47. Miele E, Spin GP, Miele E, nac , Tomao S. Albumin-bound formulation pac axel (Abraxan ABI-007) in the treatment of breast cancer. *Int J N omedicine*. 2009;4(1):99–105. doi:10.2147/ijn.s2
48. M sushita S, Chuang VTG, Kanazawa M, et al. Recombinant human um albumin mer has high blood circulation activity and low cular permea ity in comparison with native human serum al in. *Pharm es*. 2006;23(5):882–891. doi:10.1007/s11095-006-9933
Luk B, Jiang Y, Copp J, et al. Biomimetic targeting of nanoparticles e cell subsets via cognate antigen interactions. *Mol Pharm Acs*. 2018;15(9):3723–3728.
50. Eyles JL, Roberts AW, Metcalf D, Wicks IP. Granulocyte colony-stimulating factor and neutrophils—forgotten mediators of inflammatory disease. *Nat Clin Pract Rheumatol*. 2006;2(9):500–510. doi:10.1038/ncprheum0291
51. Zhang Y, Cai K, Li C, et al. Macrophage-membrane-coated nanoparticles for tumor-targeted chemotherapy. *Nano Lett Acs*. 2018;18(3):1908–1915.
52. Yu GT, Lang R, Hao W, et al. Myeloid-derived suppressor cell membrane-coated magnetic nanoparticles for cancer theranostics by inducing macrophage polarization and synergizing immunogenic cell death. *Adv Funct Mater*. 2018;28(37):1801389.